

## Current oscillations and stable electric field domains in doped GaAs/AlAs superlattices

This article has been downloaded from IOPscience. Please scroll down to see the full text article.

1997 Semicond. Sci. Technol. 12 401

(<http://iopscience.iop.org/0268-1242/12/4/010>)

[The Table of Contents](#) and [more related content](#) is available

Download details:

IP Address: 129.8.242.67

The article was downloaded on 27/11/2009 at 06:50

Please note that [terms and conditions apply](#).

# Current oscillations and stable electric field domains in doped GaAs/AlAs superlattices

Baoquan Sun, Desheng Jiang and Xiaojie Wang

National Laboratory for Superlattices and Microstructures, Institute of Semiconductors, Chinese Academy of Sciences, 100083 Beijing, People's Republic of China

Received 10 September 1996, in final form 7 January 1997, accepted for publication 15 January 1997

**Abstract.** The crossover between two regimes has been observed in the vertical electric transport of weakly coupled GaAs/AlAs superlattices (SLs). At fixed d.c. bias, the SLs can be triggered by illumination to switch from a regime of temporal current oscillation to the formation of a stable electric field domain. The conversion can be reversed by raising the sample temperature to about 200 K. An effective carrier injection model is proposed to explain the conversion processes, taking into account the contact resistance originating from DX centres in the  $n^+$ -Al<sub>0.5</sub>Ga<sub>0.5</sub>As contact layers which is sensitive to light illumination and temperature. In addition, quasiperiodic oscillations have been observed at a particular d.c. bias voltage.

Since the formation of electric field domains and related oscillations in the  $I$ - $V$  curve of superlattices (SLs) were first observed by Esaki and Chang [1], many experimental and theoretical works have been performed to investigate vertical transport properties of SLs [1–6]. In SLs with moderate carrier concentrations provided by doping or photoexcitation, low and high electric field domains occur with a charge accumulated boundary when the applied electric field is large enough to break up a uniform electric field distribution. With increasing bias voltage, the domain boundary moves through the SL and gives rise to oscillatory behaviour in the  $I$ - $V$  characteristics. The formation of electric field domains can be seen through  $\Gamma$ - $\Gamma$  sequential resonant tunnelling or  $\Gamma$ - $X$  sequential resonant tunnelling [3,4]. Recently, damped and undamped temporal self-oscillations of the current were observed in the MHz range for SLs biased by a fixed d.c. voltage [7,8]. For SLs with a certain range of doping concentration, undamped self-oscillations of the current have been reported to occur at relatively high d.c. voltage, i.e. in the second current plateau region of the  $I$ - $V$  curve. Above and below this doping concentration, the self-oscillations disappear completely, resulting in the build-up of stable electric field domains at higher doping concentrations or in a uniform electric field distribution at lower doping concentrations [9]. In the case of temporal self-oscillations, movement of the domain boundary is proposed to be responsible for the oscillations [8]. The oscillatory behaviour may possibly be employed in device applications, for example, to produce tunable microwave generators.

In this paper we show that doped SLs can exhibit either undamped self-oscillations of the current or stable electric field domains under a relatively low d.c. voltage (the first current plateau region in the  $I$ - $V$  curve). Switching between these two states is controlled by triggering the sample with additional optical illumination for the transition from current self-oscillations to stable electric field domains, and by raising the sample temperature for the transition from stable electric field domains to current self-oscillations. This behaviour is attributed to metastable transitions of DX centres in the  $n^+$ -Al<sub>0.5</sub>Ga<sub>0.5</sub>As contact layer and their influence on electron injection into the active SL region. In addition, quasiperiodic oscillations have been observed.

The samples investigated in this work were doped GaAs/AlAs SLs grown by molecular beam epitaxy in a VGMPKII system. The typical SL sample consists of 40 periods of 87 Å GaAs well and 41 Å AlAs barrier. The layer thicknesses were checked by x-ray double crystal diffraction. To reduce the density of interface states, only the centre 50 Å of the well was doped with Si ( $n = 3 \times 10^{17} \text{ cm}^{-3}$ ). The top  $n^+$  contact layer was 0.33 μm Al<sub>0.5</sub>Ga<sub>0.5</sub>As and 200 Å GaAs, doped with a Si donor concentration of  $2 \times 10^{18} \text{ cm}^{-3}$ . The area of the sample is 0.25 mm<sup>2</sup>. A 0.2 mm diameter window was processed on the top side of samples for optical illumination.

The  $I$ - $V$  characteristics of the sample were measured at 77 K under different illumination conditions, by computer-controlled data recording at a sampling frequency of 100 kHz using the pseudo-four-terminal technique (the

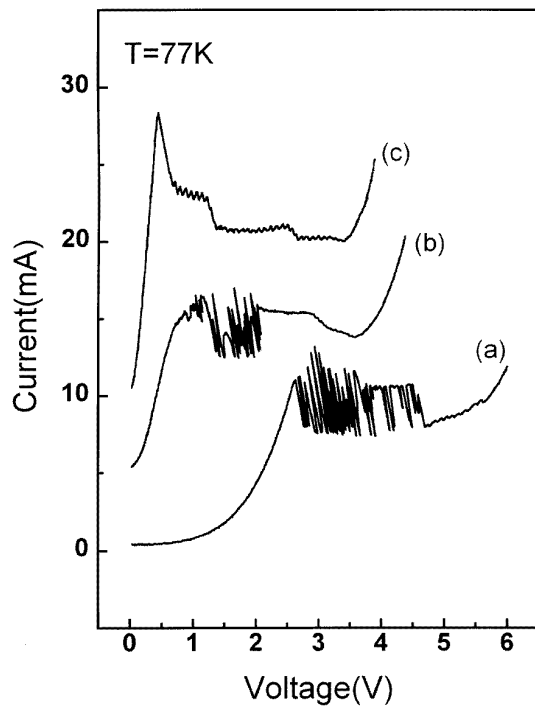


**Figure 1.** The  $I$ - $V$  characteristics of GaAs/AlAs SLs measured with a sampling frequency of 100 kHz at 77 K: (a) in the dark, (b) in background room light (shifted up 5 mA for clarity) and (c) after illumination by He-Ne laser light for 1 min (shifted up 10 mA for clarity).

negative pole is connected to the top contact layer). In addition, the usual  $I$ - $V$  curve measurement was also made with a slower scanning velocity of  $50 \text{ mV s}^{-1}$ . The temporal current self-oscillations in the MHz range were recorded by photographing the display of a Hitachi V-1050F oscilloscope, and their frequency spectra were measured by an HP859213 spectrum analyser.

The  $I$ - $V$  curves measured with a sampling frequency of 100 kHz under d.c. biasing are shown in figure 1 for the following conditions: (a) in the dark, (b) with background room light illumination and (c) after illumination with an He-Ne laser beam ( $6328 \text{ \AA}$ ,  $1 \text{ mW}$ ) for 1 min. In curve (a), the sample was cooled down to 77 K in the dark. An  $I$ - $V$  curve typical for the weakly coupled SL is observed except when d.c. voltage is applied in the range 2.6–4.6 V. An irregularly fluctuating current curve is recorded in this voltage range which results from the temporal current oscillations in the MHz frequency range and will be discussed in detail below. As shown in curve (b), when the sample is exposed to the background room light illumination, the region of irregular current fluctuation moves to the voltage range between about 0.75 and 2.0 V. Within the region of irregular current fluctuation, the temporal current oscillations can be directly observed with the oscilloscope and their frequency spectra can be analysed by a spectrum analyser. Figures 2(a), (b) and (c) display the frequency spectra and current oscillations measured at several fixed bias voltages under the conditions described in figure 1 curve (b). At a bias voltage of 1.41 V, for example, the amplitude versus

frequency relation is shown in figure 2(c). The fundamental frequency of the oscillations is located at about 1 MHz. Additionally, there are higher-order harmonics occurring due to the nonlinearity arising from the negative differential conductance (NDC) of the sample. The temporal current oscillations are attributed to a motion of the domain boundary through the SLs [8].

Under the same conditions as figure 1 curve (b), the  $I$ - $V$  characteristic is additionally measured by a slow scanning method as shown in figure 3 curve (a). Instead of exhibiting a fluctuation region, a flat portion occurs in the corresponding bias region of the  $I$ - $V$  curve, which is similar to the report by Schwarz *et al* [10]. It means that the unstable and stable electric field domains can be separated in the  $I$ - $V$  curve measured by high-frequency recording, not by slow scanning recording, i.e. the high-frequency recording can give us more information about the properties of the electric field domains.

After the sample has been illuminated by He-Ne laser light for about 1 min at low temperature, the temporal current oscillations disappear and stable electric field domains occur, as shown in figure 1 curve (c). Afterwards, if the sample is kept at 77 K, its  $I$ - $V$  characteristic remains in the same form as curve (c). However, it is found that when the sample temperature is raised up to about 200 K and then cooled once again to 77 K, the  $I$ - $V$  curve will repeat the same behaviour as shown in figure 1 curve (a), i.e. the temporal oscillations of the current will take place once again in the same bias voltage region of the  $I$ - $V$  curve. This indicates that at low temperature and fixed d.c. bias the sample may have two interchangeable states in the dark. One state exhibits the self-oscillations of current, and the other has stable electric field domains. The two states can be switched over by the trigger of light illumination (for transition from the regime of self-oscillations to stable electric field domains) and by raising sample temperature (for transition from stable electric field domains to self-oscillations). Such light illumination and temperature-sensitive properties are somehow similar to the behaviour of DX centres when  $x > 0.2$  in n-doped  $\text{Al}_x\text{Ga}_{1-x}\text{As}$  [11].

It is found that the voltage value at the first NDC peak in the  $I$ - $V$  curves is different for the cases in curves (a), (b) and (c) of figure 1. It shifts from about 2.6 V in curve (a) to 0.5 V in curve (c), depending on the conditions of the sample. Because the voltage of the first NDC peak is determined by resonant tunnelling between the ground state of adjacent wells in doped, weakly coupled GaAs/AlAs SLs [3], the large difference of bias voltage at the NDC peak should be caused by the change in the serial resistance [12]. The larger bias voltage at the NDC peak in curves (a) and (b) corresponds to a larger contact resistance of the AlGaAs electrode layer in series with the SL region. In fact, after the sample has been illuminated by laser light, the  $I$ - $V$  curve has a relatively steep rising part, as shown in curve (c) of figure 1, which is what is as expected for the conduction mechanism of resonant tunnelling between the ground state of adjacent wells, i.e. the contact resistance is small enough and can be neglected. This implies that laser illumination can metastably reduce the contact resistance of the diode and therefore enhance the electrical conductivity. Such a

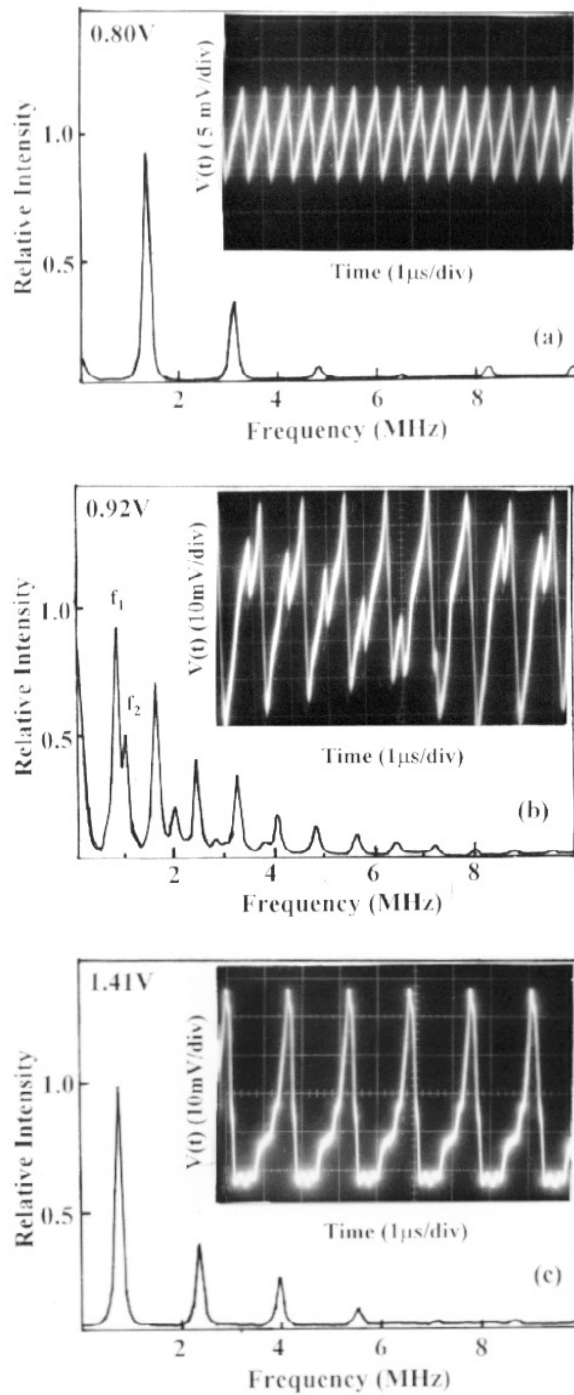


**Figure 2.** The frequency spectra of temporal current self-oscillations measured under biases of 0.80 V (a), 0.92 V (b) and 1.41 V (c). The insets depicts the time-dependent signal of the measured voltage. The sampling resistance is 30  $\Omega$ .

situation can remain even after the optical illumination has been switched off, i.e. the contact resistance has a property similar to that of persistent photoconductivity related to the DX centres in AlGaAs.

It is also found that for another GaAs/AlAs SL, with the same structure and doping densities as our typical

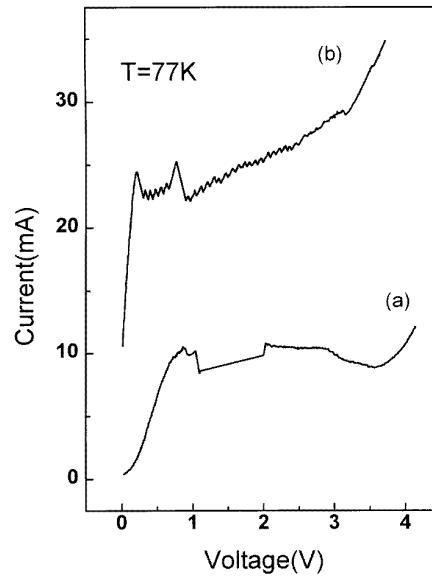


**Figure 3.** (a) The  $I$ - $V$  curve measured by a scanning velocity of 50  $\text{mV s}^{-1}$  in background room light at 77 K. (b) The  $I$ - $V$  curve of another GaAs/AlAs SL with GaAs  $n^+$  contact layer measured with a sampling frequency of 100 kHz under the conditions of curves (a) and (b) in figure 1 at 77 K (shifted up 10 mA for clarity).

sample except the top  $n^+$  contact layer is GaAs instead of  $\text{Al}_{0.5}\text{Ga}_{0.5}\text{As}$ , the high-frequency sampling measurement exhibits only stable electric field domains as shown in figure 3 curve (b) under the conditions of curves (a) and (b) in figure 1. This means that the AlGaAs contact layer plays a key role in determining whether the electric field domains are stable or unstable in the NDC region.

From the above analysis, we may attribute the switch-over between the two states of the electric field distribution in the SL to the contact resistance which controls the injection of carriers from the AlGaAs electrode into the SL region. In the case of  $N_d \sim 1.17 \times 10^{17} \text{ cm}^{-3}$ , according to our simulation calculations, the transport current should have been large enough to ensure stable electric field domain formation. However, in the case of curves (a) and (b) in figure 1 the contact resistance of the AlGaAs layers significantly restricts carrier injection into the SL region, thus the density of injected carriers is too low to form a stable field domain boundary. In fact, the average current in the self-oscillation regime (about 9 mA as shown in figure 3 curve (a)) is smaller than the average current found with stable electric field domains, about 14 mA as shown in curve (c) of figure 1 in the corresponding bias region. Thus, the smaller injected carrier concentration will cause a reduction of the effective carrier concentration  $N_d$ . However, after the deep levels of DX centres in the contact AlGaAs layer have been ionized by illumination, the serial resistance can be reduced due to the persistent conductivity. The SLs will then exhibit the behaviour of stable electric field domains.

The dependence of the temporal current oscillations on the effective carrier concentration in the SL can be clarified by a simulation using a discrete drift model calculation.

For doped, weakly coupled SLs, transport properties in the growth direction are described by the Poisson equations averaged over one SL period  $\ell$ , Ampère's equations for the balance of current density, and the voltage bias condition [6]

$$\frac{1}{\ell}(\varepsilon_i - \varepsilon_{i-1}) = \frac{e}{\epsilon}(n_i - N_d) \quad (1)$$

$$\epsilon \frac{d\varepsilon_i}{dt} + en_i v(\varepsilon_i) = J \quad (2)$$

$$\ell \sum_{i=1}^N \varepsilon_i = V \quad (3)$$

where  $\varepsilon_i$  is the average electric field,  $n_i$  is the electron concentration of the  $i$ th well and  $i = 1, 2, \dots, N$  denotes the QW index.  $\epsilon$ ,  $e$ ,  $N_d$  and  $V$  are the average permittivity, the electron charge, the average doping concentration and the applied d.c. bias voltage respectively. The total current density  $J$  is the sum of the displacement current and the electron flux due to sequential resonant tunnelling. The boundary condition at the first contact  $\epsilon(\varepsilon_1 - \varepsilon_0)/e\ell = n_1 - N_d = \delta$  allows for a small negative charge accumulation in the first well ( $\delta \ll N_d$ ). The initial conditions are  $\varepsilon_i(0) = V/N\ell$ . The velocity curve  $v(\varepsilon)$  in the NDC region is modelled by a Lorentzian curve. Combining equations (1), (2) and (3), we obtain  $N$  dimensionless equations for the electric field distributions

$$\frac{d\varepsilon_i}{dt} = \frac{1}{N} \sum_{j=1}^N v(E_j)(E_j - E_{j+1} + v) - v(E_i)(E_i - E_{i-1} + v) \quad (4)$$

and an expression for the electric current

$$J(t) = \frac{\epsilon \varepsilon_{1-1}}{N t_{\text{tun}}} \sum_{j=1}^N (E_j - E_{j-1} + v)v(E_j). \quad (5)$$

In the case of NDC induced by resonant tunnelling between the ground state of adjacent wells, equations (4) are solved numerically by the fourth-order Runge–Kutta method. For calculating the electric field distributions in the SL region under different d.c. bias voltages, the parameters used are as follows: periodic number  $N = 40$ , length per period  $\ell = 12.8$  nm, electric field strength at the NDC peak  $\varepsilon_{1-1} \approx 1.56 \times 10^4$  V cm<sup>-1</sup>, tunnelling time  $t_{\text{tun}} \approx 10$  ns. The dimensionless electron drift velocity curve  $v(E)$  used in the simulation is shown in the inset of figure 4. Using the boundary condition of a  $\delta$  value from  $10^{-1}$  to  $10^{-5}$ , we obtained a range of carrier concentrations for realizing the current self-oscillations at a fixed d.c. bias voltage of 1.41 V, as shown in figure 4. The range of carrier concentrations for displaying current self-oscillations is located from about  $0.87$  to  $2.89 \times 10^{16}$  cm<sup>-3</sup> at  $\delta = 10^{-2}$ . Therefore, the calculation shows that the average doping concentration in the sample ( $N_d \sim 1.17 \times 10^{17}$  cm<sup>-3</sup>) is high enough for a build-up of stable electric field domains in the SL region, as we observed in figure 1 curve (c). However, due to the presence of a highly resistive AlGaAs contact layer, the injection-limited effective carrier concentration should be less than the nominal value, i.e. below  $2.89 \times 10^{16}$  cm<sup>-3</sup>, which results in the temporal self-oscillations shown in curves (b) and (c) of figure 1.

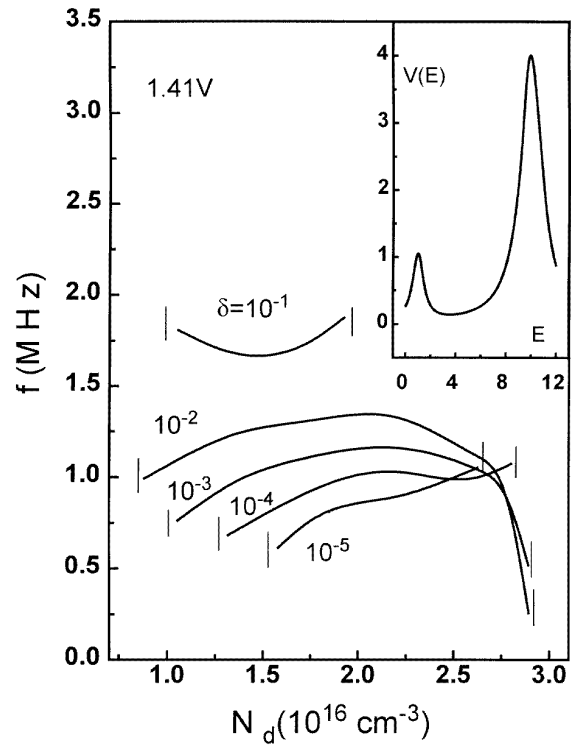


**Figure 4.** Frequency ( $f$ ) versus concentration ( $N_d$ ) calculated by the discrete drift model for different boundary parameters  $\delta$  from  $10^{-1}$  to  $10^{-5}$  at 1.41 V. The current self-oscillations disappear outside the region marked by short vertical lines. Inset: the dimensionless electron drift velocity curve  $V(E)$  used in the simulation. The two peaks correspond to the resonant tunnelling  $E_1 \rightarrow E_1$  and  $E_1 \rightarrow E_2$  respectively. They are modelled by two Lorentzian shapes.

The current self-oscillations are simulated under different d.c. bias voltages taking  $N_d \sim 2 \times 10^{16}$  cm<sup>-3</sup> and  $\delta = 10^{-3}$ . The calculated temporal current oscillations and corresponding frequency spectra are shown in figures 5(a)–(c) for three different d.c. bias conditions: (a) 0.80 V, (b) 0.92 V and (c) 1.41 V. The fundamental frequencies in these spectra are between 1.0 MHz and 2.0 MHz, decreasing with increasing bias. They are attributed to the periodic movement of the domain boundary in the SL [8]. Additionally, there are a lot of higher-order harmonics in the spectra caused by the nonlinearity related to NDC.

It is noted that the experimental results measured at 0.80 V and 1.41 V shown in figure 2 are in good agreement with the simulated ones. However, at the bias value of 0.92 V, the measured oscillations and frequency spectra are not consistent with the simulation, displaying quasiperiodic oscillations. The quasiperiodic oscillations can be attributed to a superposition of two independent periodic oscillation, as shown in figure 2(b). The fundamental frequencies are 0.8 MHz and 1.0 MHz. Thus, the SL system can be described by two independent periodic oscillation systems. This is tentatively attributed to a process leading to the creation of the chaotic window by varying the applied d.c. bias [13].

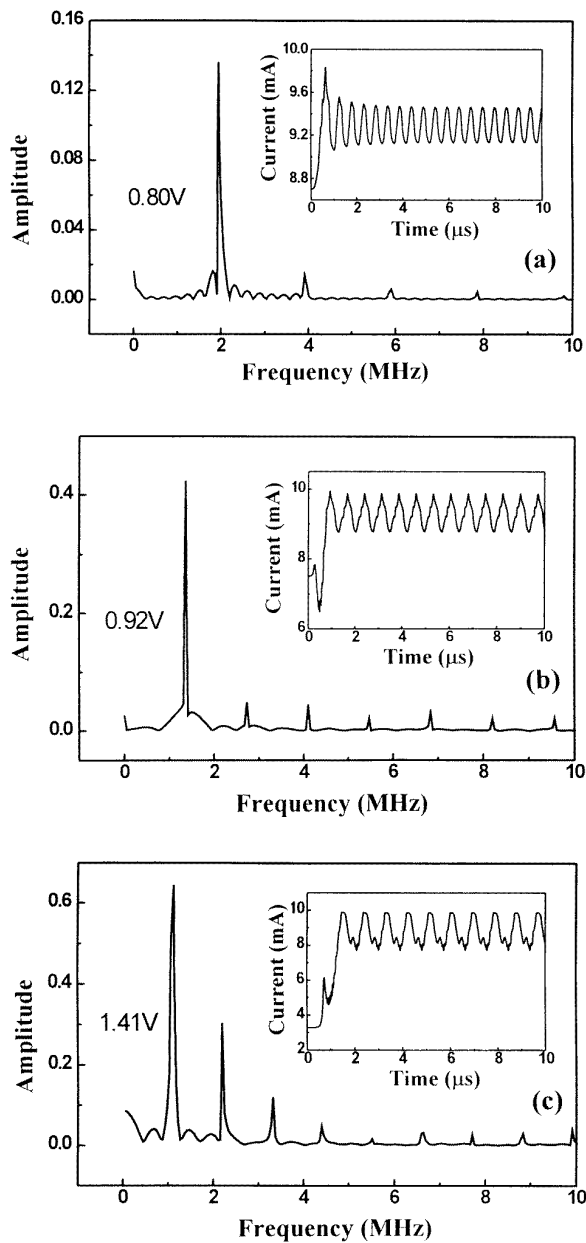


**Figure 5.** The simulated frequency spectra of temporal current self-oscillations by the discrete drift model under biases of 0.80 V (a), 0.92 V (b) and 1.41 V (c). The insets show calculated temporal current oscillations.

In summary, we have investigated the formation of current self-oscillations and stable electric field domains. The sample exhibits either temporal current oscillations at fixed d.c. bias voltage or stable electric field domains, being controlled by the illumination conditions. Switching over from temporal current oscillations to stable electric field domain formation occurs when the sample is illuminated by laser light, but the transition reverses when the temperature is raised to about 200 K and then cooled again to 77 K. The reason for the switch-over between two states is attributed to the contact resistance originating from the  $n^+$ -Al<sub>0.5</sub>Ga<sub>0.5</sub>As layers and the undersupply of injected current into the SL region. Whether the domain boundary is stable or not is determined not only by the average doping concentration, but also by the injected current when the sample has a larger contact resistance. In addition, quasiperiodic oscillations have been observed experimentally.

## References

- [1] Esaki L and Chang L L 1974 *Phys. Rev. Lett.* **33** 495
- [2] Capasso F, Mohammad K and Cho A Y 1986 *Appl. Phys. Lett.* **48** 478
- [3] Choi K K, Levine B F, Malik R J, Walker J and Bethea C G 1987 *Phys. Rev. B* **35** 4172
- [4] Zhang Y H, Yang X P, Liu W, Zhang P H and Jiang D S 1994 *Appl. Phys. Lett.* **65** 1148
- [5] Bonilla L L, Galan J, Cuesta J A, Martinez F C and Molera J M 1994 *Phys. Rev. B* **50** 8644
- [6] Bulashenko O M and Bonilla L L 1995 *Phys. Rev. B* **52** 7849
- [7] Merlin R, Kwok S H, Norris T B, Grahn H T, Ploog K, Bonilla L L, Galan J, Cuesta J A, Martinez F C and Moleara J 1995 *Proc. 22nd Int. Conf. on the Physics of Semiconductors* ed D J Lockwood (Singapore: World Scientific) p 1039
- [8] Grahn H T, Kastrup J, Ploog K, Bonilla L L, Galan J, Kindelan M and Moscoso M 1995 *Japan. J. Appl. Phys.* **34** 4526
- [9] Kastrup J, Klann R, Grahn H T, Ploog K, Bonilla L L, Galan J, Kindelan M, Moscoso M and Merlin R 1995 *Phys. Rev. B* **52** 13761
- [10] Schwarz G, Wacker A, Prengel F, Shöll E, Kastrup J, Grahn H T and Ploog K 1996 *Semicond. Sci. Technol.* **11** 475
- [11] Bourgoin J C 1990 in *Physics of DX Centers in GaAs Alloys* (Sci-Tech Publications) pp 181–94
- [12] Mendez E E and Chang L L 1990 *Surf. Sci.* **229** 173
- [13] Zhang Y H, Robert K, Grahn H T and Ploog K *Superlatt. Microstruct.* at press